ISOPHOT Observations of the Circumstellar Environment of Young Stars

P. Ábrahám

Konkoly Observatory of the Hungarian Academy of Sciences
H-1525 Budapest, P.O. Box 67, Hungary
E-mail: abraham@konkoly.hu

Abstract

ISOPHOT, the photometer on-board the *Infrared Space Observatory*, provided new photometric and spectrophotometric data on a number of pre-main sequence stars in the 2.5–200μm wavelength range. We review the capabilities of ISOPHOT for observing YSOs, briefly report on several projects related to Herbig Ae/Be, T Tau, and FU Ori-type stars, and describe our plans for compiling a homogeneous and easy-to-use photometric catalogue of all young star observations perfomed by ISOPHOT.
Keywords: *Star formation: Herbig Ae/Be stars, T Tau stars, FU Ori stars – Circumstellar matter: accretion disks – instrument: ISO, ISOPHOT – observations: photometry, spectrophotometry*

1. Introduction

In the early phases of their evolution stars are intimately linked to their environment. The spatial and density structure of their circumstellar disk/envelope can be traced by thermal emission of the dust component at infrared wavelengths. 15 years after the successful IRAS mission the *Infrared Space Observatory* (ISO, Kessler et al., 1996) provided new infrared data on the Young Stellar Object (YSO) population during its 28 months cryogenic phase.

Four years after the ISO mission, however, only part of this rich database is published and many observations are still waiting for analysis in the public ISO Archive*. This is also true for ISOPHOT, the imaging photo-polarimeter on-board ISO (Lemke et al., 1996). In many cases the original observers stopped working on their data because (i) the consolidation of the instrumental calibration took several years (and is still on-going for certain observing modes) and this timescale did not fit into the publication plan of the observers; (ii) the necessary exposure time per object turned to be longer than was anticipated prior the mission thus the target list of the proposals had to be cut back seriously.

*www.iso.vilspa.esa.es/IDA

For some proposals of statistical nature the original scientific goal became unrealistic and the observers were not interested in analysing a limited number of individual sources instead of evaluating statistical samples. All these data are freely downloadable now from the ISO Archive for analysis and publication.

In this contribution we discuss ISOPHOT observations of YSOs, with the hope of triggering new interest in the analysis of the archive data. First we review the main technical parameters of ISOPHOT, with special emphasis on the possibilities which could bring new type of information on YSOs. Then, as example, I report on several on-going or finalized YSO projects I was involved in. Finally, future plans are summarized concerning the publication of all YSO-related ISOPHOT data in a photometric catalogue. This catalogue could also be of great help in designing observations for future infrared space missions.

2. ISOPHOT's capabilities for observing YSOs

For a general description of the ISOPHOT instrument we refer to the ISOPHOT Handbook (Laureijs et al. 2002). In this section we discuss only those instrumental aspects which turned to be of special importance for YSO observations.

Photometry: multi-filter observations. The four photometric points of IRAS at 12, 25, 60, and 100μm were useful in identifying YSO candidates but were not sufficient to constrain models on morphology, mass and temperature distribution, heating mechanism and chemical composition. ISOPHOT was designed to provide SEDs in the 3.6–200μm range with much finer spectral sampling. The observer could select up to 24 filters, some of them centred on specific wavelengths, e.g. on PAH emission feaures. In practice typically not more than 4–10 filters were used (with higher preference for the broad-band continuum as well as the IRAS-compatible filters) due to time limitations. Because of the large variety of selectable observing modes, detectors, filters, and apertures, a single accuracy figure cannot be derived for ISOPHOT.

Photometry: spatial resolution. Though the mirror diameters of IRAS and ISO were identical (60 cm), ISOPHOT's design allowed to reach higher spatial resolution. It was a great advantage in observations of YSOs which are often located within dense molecular clumps. ISOPHOT's higher spatial resolution at far-infrared wavelengths was crucial to reduce contamination by the clumps' emission and obtain more precise photometry of the central source.

Shortward of 100 micron a series of apertures was available, and the one matching best the Airy-disk could be selected by the observer. In the 60–105μm range a 3×3 mini-camera could be used, whose pixel size of 43.5″×43.5″ was larger than ideal for matching the PSF (FWHM: 21″ at 60μm, 37″ at 105μm), but it represented a significant improvement compared to the 100 micron detectors of IRAS (3′×5′). At $\lambda > 105\mu$m a 2×2 camera with pixel sizes of 89″×89″ was available. Its angular resolution – dictated again by the pixel size rather than by the PSF – was 1.5′×1.5′, in the order of the IRAS 100 micron detector. Unfortunately, in many observations larger than ideal apertures were used and confusion within the beam remained one of the main limiting factors for the accuracy of far-infrared ISOPHOT observations.

There were a number of observations intended to resolve the extended envelopes of selected YSOs. Most of these measurements, however, utilized the PHT32 (oversampled) observing mode which suffered from serious instrumental problems and is still difficult to calibrate. On the other hand, observations in other modes were able to measure the size of small extended sources of 30–60″.

Mid-infrared spectrophotometry of YSOs is a good tool to detect – in addition to the continuum due to photospheric emission or to radiation of the inner warm part of the accretion disk – broad spectral features like the one of amorphous silicate around 9.7μm, the set of features attributed to PAHs (3.3, 6.3, 7.7, 8.6, 11.3μm), interstellar ices towards deeply embedded objects, the signature of crystalline silicate, etc. The grating spectrophotometer ISOPHOT-S covered simultaneously the 2.5–4.9μm and 5.8–11.6μm ranges with a spectral resolution of about 100, and delivered low-resolution spectra of young objects too faint for the higher resolution ISO-SWS instrument.

Far-infrared mapping. Star forming regions as well as the environment of YSOs could be mapped with the two far-infrared cameras. Especially the $\lambda > 100\mu$m maps are unique and provide information on molecular cloud structure, on the initial phases of star formation, and on the distribution of cold dust in the vicinity of more evolved YSOs.

Polarimetry. For completeness we mention the polarimetric capability of ISOPHOT which was used only occasionaly for young stellar objects. An example for such a programme which searched for polarization towards NGC 7538 IRS9, HH 100 IR, and L1551 IRS5 at 25 micron was presented by Wright & Laureijs (1999).

Simultaneous SED. The possibility to observe the full 3.6–200μm SED and obtain mid-infrared spectrophotometry quasi-simultaneously (within a timescale of 1-2 hours) was important for some projects looking for temporal variation of the infrared emission. As an example we refer to Sect. 3.4 where photometric observations of five FU Ori-type stars are presented.

3. ISOPHOT observations of young stars

A number of ISOPHOT observing programmes were initiated to obtain detailed SEDs of young stars. The results are usually compared with model predictions; first of all with the expected spectral shape of a geometrically-thin, optically-thick circumstellar disk ($\lambda F_\lambda \propto \lambda^{-4/3}$). Deviations from this shape are interpreted in terms of structural changes in the circumstellar matter: deficiency at near-infrared wavelengths may indicate an inner hole while a too high far-infrared flux (which is typically the case) is the signature of a flared outer disk or of an envelope. Low-density gaps dynamically cleared by companions cause dips in the SED at the corresponding wavelengths.

3.1. Far-infrared photometry of Herbig Ae/Be stars

Herbig Ae/Be stars represent the pre-main sequence evolutionary phase of intermediate mass (2–8 $M_\odot$) stars. We observed 7 of these stars to deduce the structure of their circumstellar matter from the SEDs (Ábrahám et al. 2000). Since Herbig Ae/Be stars are often embedded in dense molecular clumps ISOPHOT's higher spatial resolution at far-infrared wavelengths was crucial to reduce contamination by the clumps' emission. Fig. 1 presents our results for two stars.

The SED of LkHα 233, composed of ISOPHOT and IRAS photometry as well as data from the literature, can be described by a power-law in the 5–60μm range. The peak of the SED was predicted at around 100μm by the earlier IRAS measurement, but our 90μm photometry showed that the larger beam of IRAS was contaminated at this wavelength and the circumstellar region of LkHα 233 contains mainly material warmer than 90 K (see Fig. 1). A high resolution ISOPHOT scan at 150μm (not presented here) supports this result by detecting only the clump with no indication for the star. These results fully support a geometrically thin accretion disk model for LkHα 233 as proposed by Leinert et al. (1993).

The other Herbig Ae/Be star, MWC 1080, shows a completely different SED: the flux density is constant in the mid-infrared but the spectrum exhibits a steep raise starting between 20 and 25μm as revealed by the ISOPHOT data

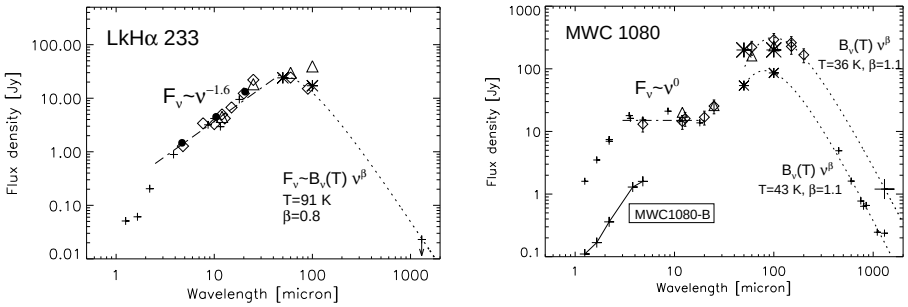

Figure 1: Spectral energy distributions of 2 Herbig Ae/Be stars. *Diamonds:* ISOPHOT; *dots:* UKIRT/MAX; *triangles:* IRAS; *small plus signs and asterisks:* ground-based and KAO observations of small beam size; *large plus signs and asterisks:* ground-based and KAO observations of large beam size (from Ábrahám et al. 2000).

points at these two wavelengths. The strong emission peak centred at 100μm has been thought to originate from the circumstellar region of the star. The typical temperature of the emitting material, however, is almost the same in the large 3′ beam of ISOPHOT and in the smaller ∼20″ aperture used in several KAO and SCUBA observations. The lack of temperature gradient towards the central source indicates that the heating of the emitting dust is independent of MWC 1080, and is more likely due to the embedded cluster of stars seen on K-band images around the Herbig star. Thus models of the circumstellar structure of MWC 1080 do not have to reproduce the far-infrared peak of the SED which is to a large extent unrelated to the central source. The true far-infrared spectrum of MWC 1080 at $\lambda > 20\mu$m cannot be determined from our observations because it would require a significantly higher spatial resolution than available at the moment.

3.2. Circumstellar structure of T Tauri stars

In an on-going project we are studying 34 T Tauri-type stars by analysing their 3.6–200μm SEDs composed of 8–12 ISOPHOT photometric bands. More than half of the sample consists of binary stars. Our goals are twofold: (1) taking advantage of the unprecedented filter coverage of ISOPHOT we determine a detailed SED and compare it with models, e.g. the ones proposed by Chiang & Goldreich (1997); (2) in a young binary system the evolution of the circumstellar disks may depend on the separation and the orbits of the components. Sorting

the binaries in our sample according to the separation of their components and looking for systematic changes in the shape of their SEDs we could shed some light on the size and structure of the circumstellar disks in binary systems. Since the flux density of T Tau stars typically varies within one order of magnitude in the whole infrared range, this comparison requires photometric accuracies around 10% which is a challenge even to the present calibration of ISOPHOT. On the other hand contamination in the beam is less problematic than in the cases of Herbig Ae/Be stars, since T Tau stars are usually not able to heat up their environment creating an extended emitting area around the source.

In Fig. 2 we present some preliminary results. The SED of AK Sco, a binary system, is an example for a rather typical case: the infrared excess emission follows a power-law in the 15–60μm range and peaks around 60μm. At longer wavelengths the emission drops quickly demonstrating the lack of a significant amount of cold dust in the system. The environment of MWC 863 is probably different from that: the emission peak at 20μm indicates a higher average dust temperature, i.e. the outer part of the accretion disk seems to be completely missing. The SED of LkHα 332-20 is virtually very noisy. However, the high flux around 10μm originates from a strong silicate emission feature, and the alternation of peaks and dips at 25, 60, and 100μm are reproduced by the earlier IRAS data, too. Thus the relatively low 60μm emission might be a signature of a low-density ring in the disk.

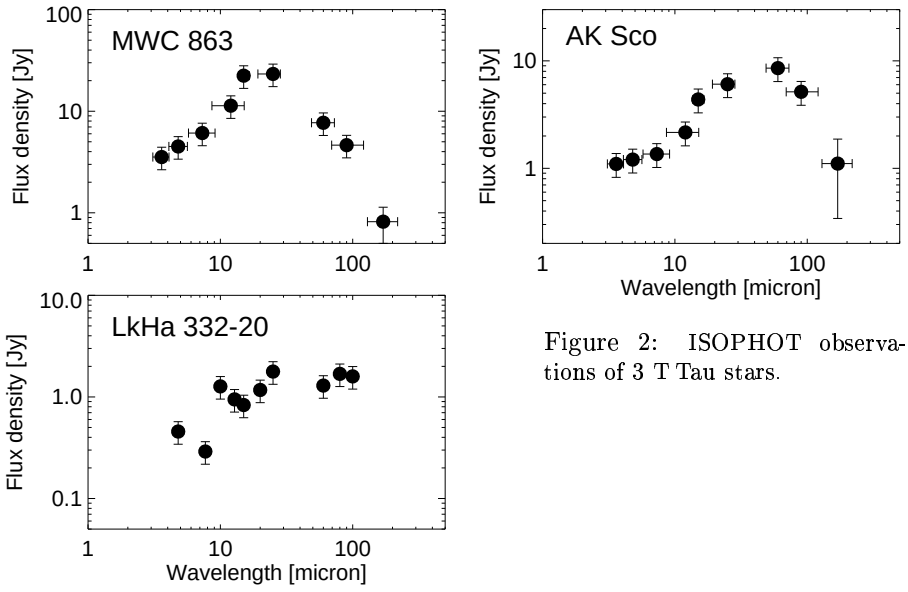

Figure 2: ISOPHOT observations of 3 T Tau stars.

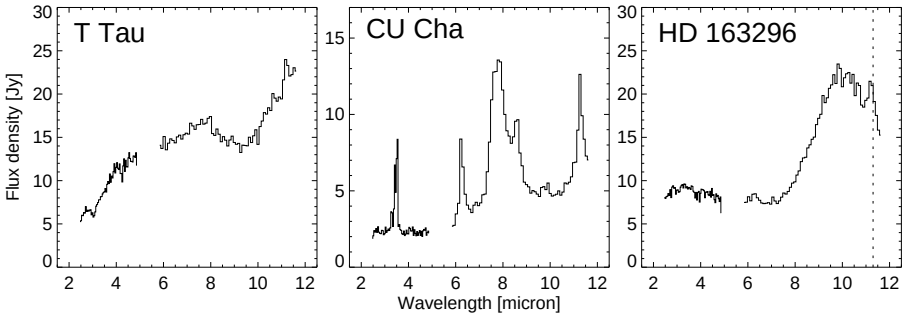

Figure 3: Mid-infrared spectrophotometry of 3 YSOs. T Tau exhibits a strong silicate absorption at 10μm, probably due to the infrared component T Tau-S. CU Cha, an A0-star, emits enough UV photons to excite PAH molecules. In HD 163296 the weak emission feature at 11.3μm on top of the strong 10μm amorphous silicate emission was also observed by ISO-SWS and is attributed to the presence of crystalline silicate.

3.3. Mid-infrared spectrophotometry of YSOs

During the ISO mission the ISOPHOT-S subinstrument performed about 90 observations on YSOs. We are working on an atlas including all these measurements. The atlas will contain 23 observations of embedded objects, 26 spectra of T Tau stars, 17 intermediate-mass pre-main sequence stars, as well as repeated observations of several FU Ori, EX Lup, and UX Ori-type objects. Fig. 3 shows three spectra as examples.

3.4. Evolution of FU Ori-type stars as seen by ISOPHOT

An FU Ori outburst is defined as a dramatic increase in the brightness of a T Tauri-type star (ΔV=4–6 mag). Since the phenomenon is connected to the circumstellar medium (probably caused by the increased accretion rate) the infrared emission spectrum is also expected to change during and after the outburst. The wavelength dependence of the change – which has never been observed before – provides crucial information on this physics of the phenomenon.

We studied 5 FU Ori stars and compiled their SEDs from the ISOPHOT data supplemented with other (2MASS, MSX, etc.) observations performed during the ISO mission (1995-98). These SEDs were compared with 15 years earlier ones derived from the IRAS photometry as well as from ground-based observations carried out around 1983. In 3 cases no difference between the two epochs was seen within the measurement uncertainties, but in one case the

shorter wavelength part of the spectrum ($\lambda \leq 20\mu$m) has decreased by a factor of 2, and in the 5th case a marginal fading was observed. The definite case (V1057 Cyg) shows wavelength-independent fading below 20μm, indicating that the energy source of the inner part of the disk is more re-processed starlight than accretion luminosity. We plan to analyse also similar observational sequences of several other FU Ori and EX Lup type stars.

4. Future work

At Konkoly Observatory we plan to collect and publish all YSO observations of ISOPHOT in a photometric catalogue which, together with the ISOPHOT-S spectral atlas, could be part of ISOPHOT's heritage in the field of star formation. In the catalogue also size of the objects and predicted confusion noise will be included. The database will serve as input catalogue for proposals for future infrared instruments like SIRTF and Herschel.

Acknowledgements

This work has been partly supported by Hungarian Research Fund (OTKA T037508). P.Á. acknowledges the support of the Bolyai Fellowship.

References

Ábrahám, P., Leinert, Ch., Burkert, A., et al., 2000, A&A 354, 965
Chiang, E.I., Goldreich, P., 1997, ApJ 490, 368
Kessler, M.F., Steinz, J.A., Anderegg, M.E., et al., 1996, A&A 315, L27
Laureijs, R.J., et al., 2002, The ISO Handbook Vol. IV, ESA SAI-99-069/Dc, Ver.2.0
Leinert, Ch., Haas, M., Weitzel, N., 1993, A&A 271, 535
Lemke, D., Klaas, U., Abolins, J., et al., 1996, 1996, A&A 315, L64
Wright, C.M., Laureijs, R.J., 1999, ESA-SP 435, 49